MICROSCOPIC DIFFUSION ANISOTROPY IMAGING: AN EX-VIVO HYPOMYELINATION MOUSE STUDY

Enrico Kaden[1], Nathaniel D Kelm[2], Robert P Carson[3], Mark D Does[2], and Daniel C Alexander[1]

[1]*Centre for Medical Image Computing, University College London, London, United Kingdom,* [2]*Institute of Imaging Science, Vanderbilt University, Nashville, TN, United States,* [3]*Departments of Neurology and Pediatrics, Vanderbilt University, Nashville, TN, United States*

Target audience. Researchers interested in diffusion MRI, especially biophysical model development, statistical data analysis, and hypomyelination mouse models.

Purpose. The diffusion MR signal is sensitive to tissue properties in the range of few micrometres, such as the size of cells and their extensions (e.g., dendrites and axons, also known as neurites), the degree of myelination, and the space between neurites, averaged over a large population of micro-environments with potentially complex orientation distribution. This work proposes a new method, which we call spherical mean technique (SMT), for estimating the microscopic diffusion anisotropy unconfounded by neurite orientation dispersion and crossing, which are ubiquitous in the brain. A distinguishing feature of the method is that it does not rely on complex diffusion sequences with multiple gradient pulses or magic-angle spinning. We will demonstrate SMT in an ex-vivo mouse brain study and its capability for detecting hypomyelination conditions.

Theory. First we model the diffusion signal $h_b(g, \omega) = \exp(-b\,\langle g, \omega\rangle^2\,\lambda_{\parallel})\,\exp(-b\,(1-\langle g, \omega\rangle^2)\,\lambda_{\perp})$ for a micro-environment up to its orientation using a second-order approximation, where b denotes the diffusion weighting factor and ω the gradient direction. $\lambda_{\parallel}$ and $\lambda_{\perp}$ quantify the microscopic diffusivities parallel and perpendicular to the micro-domains, which we aim to recover in this work. The spherical convolution of h_b with the orientation distribution yields the MR signal observable on the voxel scale[1]. The key observation is that for a fixed b-value the spherical mean of the diffusion signal over the gradient directions does not depend on the orientation distribution. More specifically, the mean signal $\bar{e}_b(\lambda_{\parallel}, \lambda_{\perp}) = \exp(-b\,\lambda_{\perp})\;{}_1F_1(1/2;\,3/2;\,-b\,(\lambda_{\parallel}-\lambda_{\perp}))$ is only a function of the microscopic diffusion coefficients, where ${}_1F_1$ denotes the confluent hypergeometric function. This approach is related to the powder average[2,3]: We measure the diffusion signal uniformly over all gradient directions while the other sequence parameters are kept fixed, which is carried out for two or more b-shells to enable the estimation of $\lambda_{\parallel}$ and $\lambda_{\perp}$ from the $\bar{e}_b$'s.

Methods. To show the utility of SMT, we study two animal models, Rictor and tuberous sclerosis complex (TSC) conditional knock-out mice[4,5], which result in moderate (Rictor) and severe (TSC) hypomyelination. Eight normal, five Rictor, and five TSC P60 mouse brains were measured ex vivo on a 15.2 T Bruker scanner using a 3D diffusion-weighted fast-spin-echo sequence with TR/TE/ESP = 200/19.0/7.1 ms and ETL = 4. At an isotropic voxel resolution of 150 µm we acquired two b-shells with b = 3000, 6000 s/mm² (δ/Δ = 5/12 ms) and 30 gradient directions each (twice with gradient polarity reversed), in addition to 5 zero b-value images[6]. The scan time was about 12 h. After image reconstruction from the k-space data and gradient non-linearity correction we calculated the mean signal $\bar{e}_b$ for each b-shell and estimated the microscopic diffusivities $\lambda_{\parallel}$ and $\lambda_{\perp}$. Moreover, we chose a normal brain from the control group as reference, to which all other subjects were transformed using non-linear registration as implemented in FSL (Oxford).

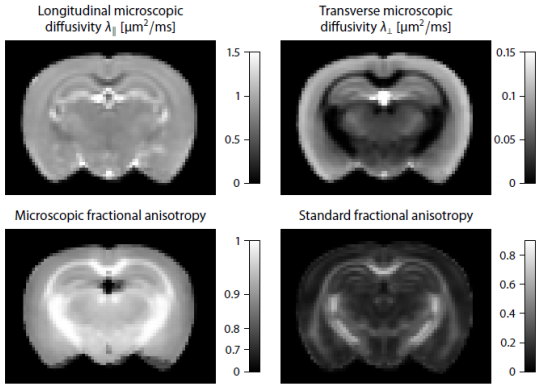

Figure 1: Control group average.

Results. Figure 1 (top row) depicts the longitudinal and transverse microscopic diffusion coefficients averaged over the control group of normal brains. In the bottom panel we compare the micro-domain fractional anisotropy (FA), which is computed from $\lambda_{\parallel}$ and $\lambda_{\perp}$, with the FA measure derived from the classical tensor model. The key difference is that the former metric has factored out the effects due to orientation distribution. The two upper rows in Figure 2 show the voxel-wise group difference between TSC and control mice as well as the significance of the observed differences (FWE-corrected p-value). Finally, we delineated three regions of interest, i.e., anterior commissure (AC), corpus callosum (CC), and internal capsule (IC), in the average mouse brain shown in Figure 1. The bottom section of Figure 2 depicts a region-based group analysis for Rictor vs control and TSC vs control mice using a two-sample unpaired t-test (significance codes: 0 '***' 0.001 '**' 0.01 '*' 0.05 '°' 0.1 ' ' 1).

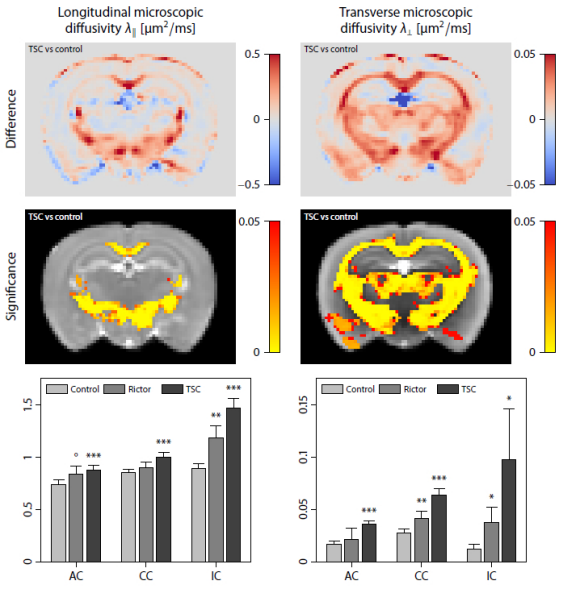

Figure 2: Group difference analysis.

Discussion. The present work has introduced SMT to disentangle microscopic diffusion anisotropy from the intra-voxel directional heterogeneity, providing markers that are not affected by orientation dispersion to study microstructural tissue features. SMT uses a widely available off-the-shelf pulse sequence with two or more b-values and high angular gradient resolution, hence this technique can be easily adopted in the clinical domain. Furthermore, we have demonstrated that the simple-to-estimate parameters are sensitive to myelination in white matter. The ex-vivo rodent study suggests that the transverse microscopic diffusivity is significantly higher in hypomyelinated mouse brains.

Acknowledgements. The UK EPSRC funded this work with grant EP/G007748.

References. [1] von dem Hagen and Henkelman, *Magnetic Resonance in Medicine*, 48:454–459, 2002. [2] Callaghan et al., *Biophysical Journal*, 28:133–142, 1979. [3] Price, *Concepts in Magnetic Resonance*, 9:299–336, 1997. [4] Carson et al., *Neurobiology of Disease*, 45:369–380, 2012. [5] Carson et al., *Human Molecular Genetics*, 22:140–152, 2013. [6] Kelm et al., *ISMRM* 979, 2014.